Smart Surface Design for Efficient Ice Protection and Control

Edited by
Carlo Antonini
Irene Tagliaro

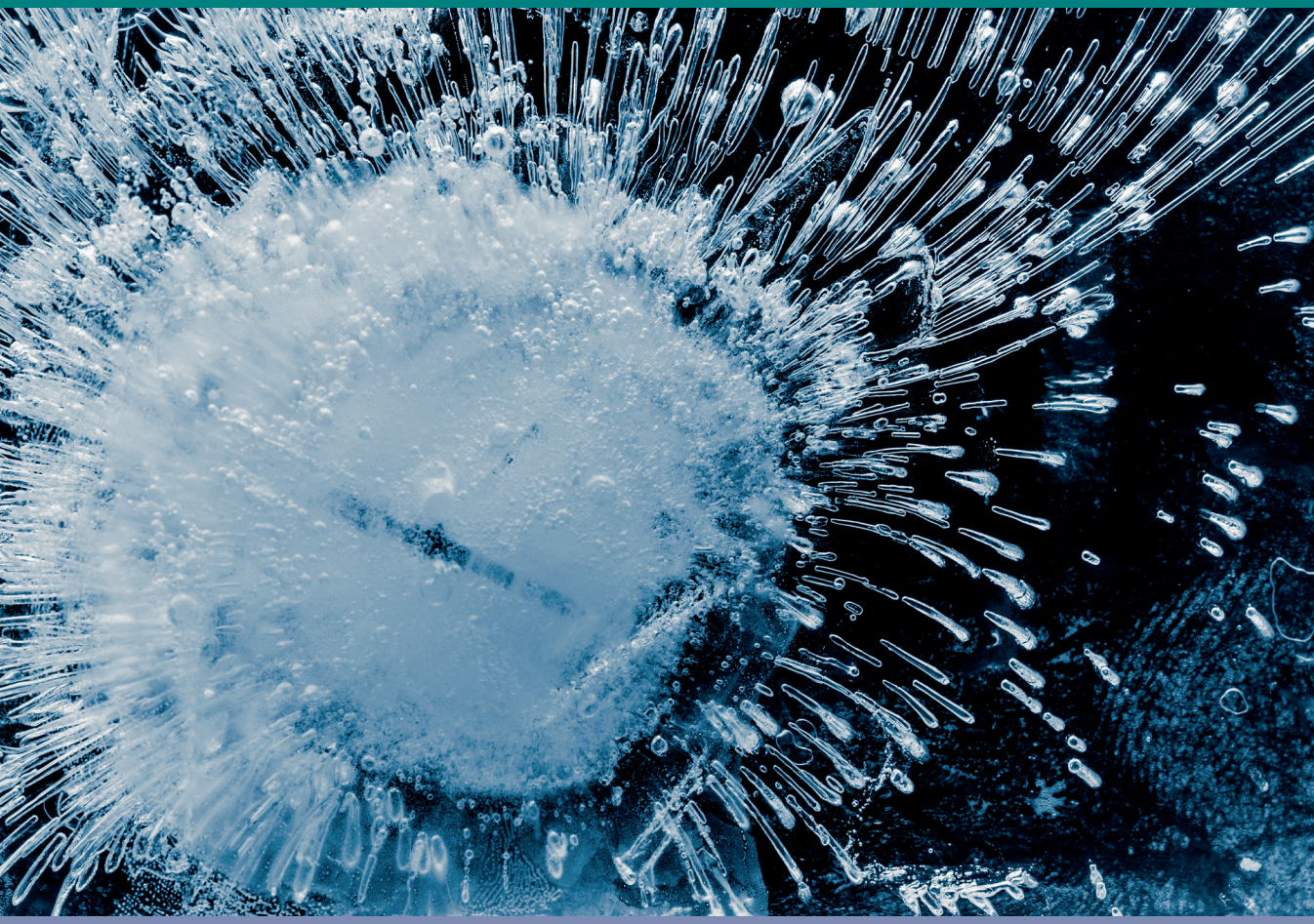

IOP | ebooks

Smart Surface Design for Efficient Ice Protection and Control

Online at: https://doi.org/10.1088/978-0-7503-6009-8

Smart Surface Design for Efficient Ice Protection and Control

Edited by
Carlo Antonini
Department of Materials Science, University of Milano-Bicocca, Milan, Italy

Irene Tagliaro
Department of Materials Science, University of Milano-Bicocca, Milan, Italy

IOP Publishing, Bristol, UK

Carlo Antonini and Irene Tagliaro have asserted their right to be identified as the editors of this work in accordance with sections 77 and 78 of the Copyright, Designs and Patents Act 1988.

ISBN 978-0-7503-6009-8 (ebook)
ISBN 978-0-7503-6007-4 (print)
ISBN 978-0-7503-6010-4 (myPrint)
ISBN 978-0-7503-6008-1 (mobi)

DOI 10.1088/978-0-7503-6009-8

Version: 20250601

IOP ebooks

British Library Cataloguing-in-Publication Data: A catalogue record for this book is available from the British Library.

Published by IOP Publishing, wholly owned by The Institute of Physics, London

IOP Publishing, No.2 The Distillery, Glassfields, Avon Street, Bristol, BS2 0GR, UK

US Office: IOP Publishing, Inc., 190 North Independence Mall West, Suite 601, Philadelphia, PA 19106, USA

IOP Publishing

Smart Surface Design for Efficient Ice Protection and Control

Carlo Antonini and Irene Tagliaro

Chapter 8

The use of thermally activatable adhesion promoters for permanent and durable immobilization of non-reactive polymeric coatings

Alexandros A Atzemoglou, Niccolò Bartalucci, Anny C Ospina Patiño, Carlo Antonini, Santiago J Garcia, Mark W Tibbitt, Samuele G P Tosatti and Stefan Zürcher

The problem of ice formation and accumulation on surfaces negatively impacts many aspects of daily life. Current strategies focus on the development of icephobic coatings that aim to repel water droplets and reduce the adhesion of ice. To function properly, icephobic coatings often require complex synthesis steps to be immobilized on surfaces, and permanent bonding with a substrate after synthesis is often not feasible. As the adhesion strength of coatings constitutes an important property that determines the performance and durability of adhesive coating systems, we immobilized polymers on different types of substrates with the use of an adhesion promoter to assess their adhesion strength. For that, lap shear tests were used to assess the adhesive bond strength of bound samples, using cyclic olefin copolymers (COCs) or epoxy as adhesives. The use of an adhesion promoter layer, capable of forming covalent bonds with any neighboring C–C bond via nitrene insertion, can increase the adhesion between materials that do not possess inherent chemical affinity, therefore creating an appropriate coating platform for adhesives that would not bind otherwise. Thermal curing of the samples with adhesion promoters containing the reactive 4-azido-3,5-difluorophenoxy (DFPxA) moiety led to increased adhesion strength. Additionally in this work, we immobilized different commonly used polymeric materials as monolayers on an aluminum substrate with the use of an adhesion promoter layer containing the reactive DFPxA moiety. Dynamic contact angle (dCA) and x-ray photoelectron spectroscopy (XPS) were used to assess the successful bonding of the reactive moiety with a wide range of different polymeric materials, demonstrating its universal attachment to neighboring

doi:10.1088/978-0-7503-6009-8ch8

bonds. Moreover, we investigated the adhesion strength of ice on immobilized monolayers of the coated polymeric films, which would not bind otherwise, revealing a correlation between adhesion strength and surface wettability.

8.1 Adhesion promoter compounds in surface engineering

Each material possesses unique characteristic properties that make it suitable for specific applications. However, there are instances where the inherent properties of a material may not fulfill certain requirements [1]. Thus, approaches to combine functionalities originating from various materials to accomplish a desired performance are needed [2, 3].

The surfaces of materials play crucial roles in applications in numerous fields as they define the interaction of a material with the surrounding environment [4]. In the field of surface engineering, polymeric coatings constitute a primary approach to modify surfaces to introduce desired functionalities without compromising the properties of the underlying bulk material [5–7]. Permanent deposition of coatings is therefore important for long-term stability and durability, since otherwise the coatings when exposed to harsh environmental conditions and without strong adhesion may peel off or delaminate, leading to premature failure and loss of protection for the substrate [8–10]. Polymeric coatings are widely used as they offer increased flexibility due to the wide range of properties that are achieved using films with different chemistries, thicknesses, and processing conditions [11]. An inherent property of amorphous polymers is the transition from a hard, glassy state to a softer rubbery state [12, 13]. Many polymers exhibit a glass transition temperature at approximately 100 °C [14–16] and when used as substrates the methods used for surface modification are limited by this property.

Nevertheless, efficient and permanent surface modifications to acquire desired surface functionalities are not always straightforward and can require time-intensive and complex processes that require in-depth analysis of the material surface chemistry [17, 18]. This is because not all polymeric materials that act as coatings have chemical affinity with multiple different substrates. The use of intermediate layers, called primers or adhesion promoters, can facilitate generalizable coating protocols of surfaces with polymeric layers [19]. More specifically, versatile adhesion promoters are bifunctional materials that can strongly bind both to various underlying substrates and covalently to arbitrary polymeric coatings, by using thermally or photolytically activated reactive groups, such as azides [20]. Thus, their use is of great benefit as they can increase adhesion between surfaces that would not bind otherwise. Aryl azides are considered stable reactive compounds, which are easy to synthesize and can form adhesion promoters for effective permanent immobilization of polymers through C–H insertion reactions [21], see figure 8.1.

To overcome these limitations, we designed and synthesized aryl azide containing adhesion promoters for versatile surface modification at temperatures below 100 °C. We focused on demonstrating the versatility of a reactive adhesion promoter towards effective binding with multiple polymers of different wettability. Further, we investigated the ice adhesion strength on the coated polymeric monolayers,

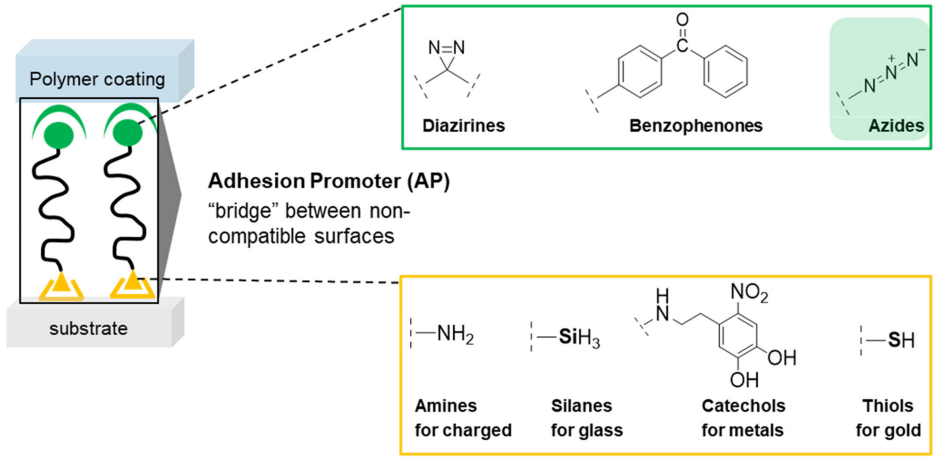

Figure 8.1. Bifunctional adhesion promoters containing aryl azides work as a chemical 'bridge' for surfaces that do not exhibit chemical affinity and would not bind otherwise. (Adapted from [77].)

presuming that thermal and elastic effects deriving from the substrate will be eliminated using a monomolecular polymeric layer tethered to the surface by another adhesion promoting monolayer. Moreover, we investigated the influence of an activated adhesion promoter on making a coating system more robust and durable, a crucial factor to avoid premature failure.

The findings we present could evolve the versatile surface modification of materials either with peculiar shapes, as well as materials that would deform when heated above 100 °C or when UV activation is not feasible.

In our previous work [22], we were able to design and synthesize reactive compounds containing aryl azides, where the activation of the azide can occur thermally already at temperatures below 100 °C. These moieties were capable of undergoing insertion reactions with a polymeric material in close proximity for efficient permanent surface modification, rendering them appropriate candidates for adhesion promoters that are to be used on materials sensitive to light or on polymers having low glass transition temperatures and low melting points. The most reactive synthesized compound was an o,o-difluoro substituted p-phenoxy azide (DFPxA moiety) and the important novelty was that the activation barrier was lowered to ~70 °C. This newly synthesized compound was compared to the commercially available perfluorophenyl azide (PFPA moiety) known to decompose at temperatures higher than 120 °C.

Based on the synthesized aryl azide compounds, we formulated adhesion promoters to assess their efficiency to create a stable chemical 'bridge' between materials that lack reactive end groups, and thus allowing for versatile and permanent surface modification. The differently substituted heat sensitive aryl azide moieties were grafted to different units that allowed for effective surface immobilization. The adhesion promoter containing the DFPxA moiety activated and successfully covalently bonded to polymer films at the lowest temperature, at ~70 °C. Thus, the fact that the

compounds can be activated at a lower temperature, especially those containing the DFPxA moiety, render them suitable adhesion promoters for permanent immobilization of coatings on polymeric materials with low glass transition temperature or low melting point, on materials with peculiar shapes or light-blocking materials where light activation is challenging or impossible.

8.2 The effect of surface-tethered monomolecular thin film wettability on ice adhesion

8.2.1 Introduction

The formation and accumulation of ice on exposed surfaces is associated with detrimental impacts on the safety and operation performance of instruments and facilities in various industries, such as aircraft [23, 24], power lines [25], off-shore platforms, wind turbines, and solar panels [26]. For safety critical applications, such as in aircrafts, de-icing methods include energy inefficient electric heating and the time-consuming application of de-icing fluids, which are environmentally problematic [27, 28]. A more appealing and universal approach is the development of economical coatings to which ice minimally adheres or can be easily removed under its own weight or due to natural factors, such as wind. This would have broad applications improving the safety and reliability of low temperature operations [29]. In order for ice to debond by natural forces or vibration, the ice adhesive strength should decrease to less than 100 kPa [30].

Understanding the mechanisms of ice adhesion and the underlying surface properties for minimizing ice–substrate interactions would enable the successful design of coatings known as 'icephobic' coatings [31–34]. Typically they leverage functionalities such as superhydrophobicity to repel water droplets, delay ice nucleation, and reduce ice adhesion significantly [35] and they are meant to be combined with de-icing strategies.

Alongside surface morphology, ice adhesion strength is commonly associated with the surface water wettability/hydrophobicity. However, there have been contradicting findings regarding the effect of surface wettability on ice adhesion strength, with some studies suggesting a decrease in ice adhesion strength on high contact angle surfaces due to their low surface energy [36, 37], whereas others have found little relation between the two parameters [29, 38, 39]. This discrepancy suggests that the relationship between water contact angle and ice adhesion strength is complex and varies depending on additional surface properties.

The design of highly structured icephobic surfaces usually requires complex protocols and modifications of the surface chemistry. Moreover, coating monolayers of polymers exhibiting icephobic properties is not feasible on substrates without chemical affinity since any physisorbed coating would likely wash off during rinsing. Here, we demonstrate the potential of an adhesion promoter carrying a low temperature activated aryl azide, which was functionalized with a nitro-catechol group, to successfully function as an intermediate for the permanent surface modification of aluminum substrates with different polymeric coatings.

Catechol-functionalized polymers covalently link to metallic substrates, via the formation of coordinate bonds with their oxides and hydroxides. However, multi-functional, cross-linked polymeric films are often formed due to the self-oxidation of the catechol moieties [40]. In order to repeatedly obtain a monomeric catechol film, Zürcher *et al* demonstrated that the introduction of electron-withdrawing groups, such as nitro groups, is required [41].

Since the adhesion promoter covalently binds both to the aluminum substrate through the nitro-catechol and to the deposited polymers through the insertion of the nitrenes, increased adhesion and stability can generally be achieved. In that manner, any structural, mechanical, or thermal effects caused by the substrate to the polymeric coating is eliminated. This way the actual chemical and physical composition of the polymer molecules are assumed to be the sole affecting factors of ice adhesion, and thus the measurements. In that respect, understanding the behavior of different classes of polymeric materials towards icing is critical and thus the force necessary to detach ice formed on a surface was measured, using a custom-made test rig to perform the horizontal shear tests.

Dynamic contact angle (dCA) and x-ray photoelectron spectroscopy (XPS) were used to assess the successful bonding of the reactive moiety with a wide range of different polymeric materials, demonstrating its universal attachment to neighboring bonds.

8.2.2 Results and discussion

Different polymeric materials were chosen based on their hydrophilicity to assess the ice adhesion strength once applied as thin, monomolecular films on an aluminum substrate (figure 8.2). Surface qualitative and quantitative characterization was performed with dCA and XPS to evaluate the successful coating mediated by an adhesion promoter consisting of a nitro-catechol and of a DFPxA reactive moiety (figure 8.3(a)). For polymeric substrates a polyethylenimine (PEI) based AP functionalized with DFPxA was synthesized (figure 8.3(b)). The elemental composition of a very thin surface layer of approximately up to 10 nm was determined using XPS [42].

Different polymeric materials of various molecular weights were tested, and the choice was based on the degree of hydrophilicity, since multiple studies suggest decrease of ice adhesion strength with low surface wettability [36, 37]. By testing a wide range of materials, the binding ability towards insertion on non-specific bonds could be demonstrated.

8.2.2.1 Aluminum characterization and deposition of the adhesion promoter

The reference substrate material chosen was aluminum alloy Al6082, a relevant material for aerospace applications, since the parts on airplane wings requiring anti-icing surfaces are usually made of Al6082 [43]. Next, the adhesion promoter used was based on the reactive DFPxA moiety, which was functionalized with a nitro-catechol end group for single site attachment to the Al6082 substrate (figure 8.3(a) and figure 8.4).

The freshly cleaned substrates were characterized by a high surface energy/low contact angle (figure 8.5) and the presence of elemental aluminum (Al), oxidized Al,

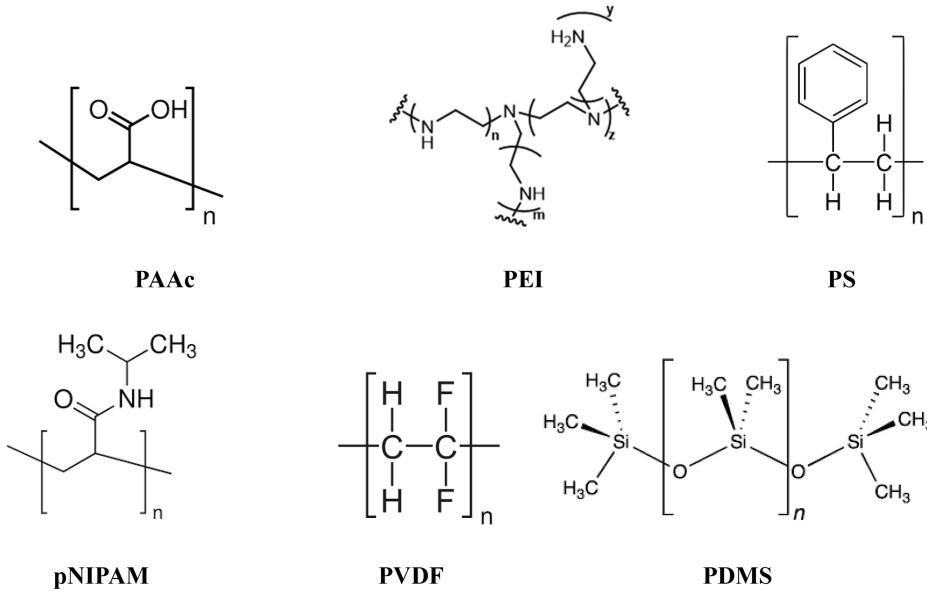

Figure 8.2. The proposed polymeric materials and their respective molecular structures, to test the binding efficacy with the ND-DFPxA adhesion promoter layer. (Adapted from [77].)

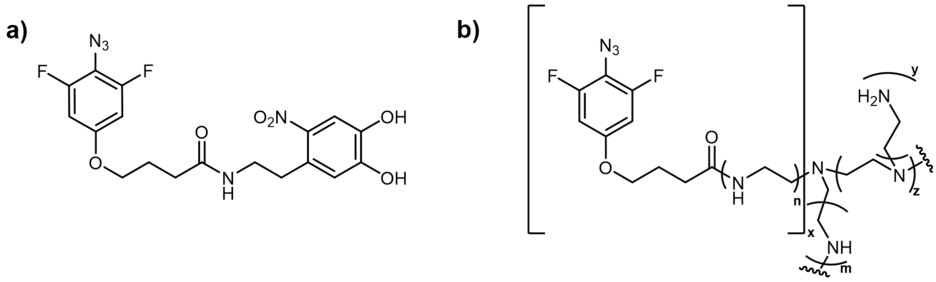

Figure 8.3. 4-azido-3,5-difluorophenoxy moiety functionalized with (a) nitrodopamine to act as an adhesion promoter compound for aluminum substrates (ND-DFPxA) and (b) polyethylenimine for glass fiber and polypropylene substrates (PEI-g-DFPxA). (Adapted from [77].)

oxygen (O), magnesium (Mg), and carbon (C) of adventitious contamination (table 8.1). Moreover, as expected in aluminum substrates due to their complex fabrication [44], a small amount of fluorine contamination was detected, as well as traces of silicon. No other elements, specifically nitrogen, were detected. The successful deposition of the adhesion promoter onto Al substrates was confirmed by an increase in carbon, the presence of nitrogen and fluorine, and the subsequent decrease of aluminum and oxygen as a consequence of attenuation of substrate photoelectrons through the adhesion promoter layer. Upon subtraction of the aluminum, as well as the aluminum and magnesium oxide contributions, the film composition of the adhesion promoter differed from the theoretically calculated

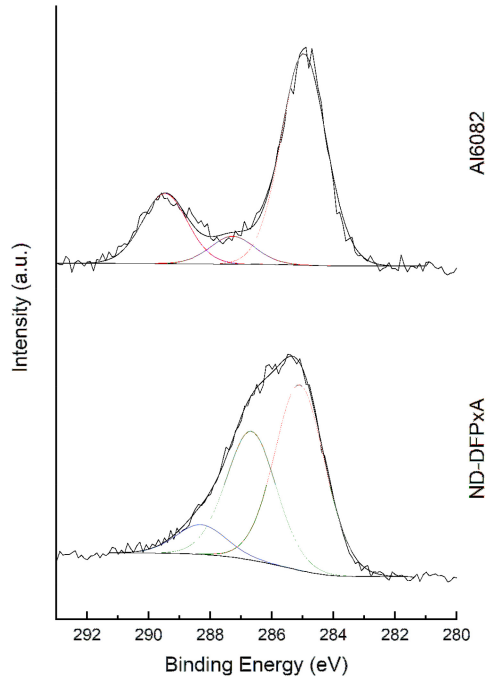

Figure 8.4. Detailed XPS spectra of the C 1s region on the bare Al6082 before and after deposition of the adhesion promoter. Curve-fitted carbon component C–C, in red; C–N, C–O in green; C–F, C=O in blue; and O–C=O in purple. (Adapted from [77].)

stoichiometry. The main deviation was an increased oxygen content, which was attributed to aluminum surface hydroxyl groups. Due to the presence of the DFPxA groups, an increase in advancing contact angle value of 58° with respect to the 14° contact angle of the bare Al substrate was also observed (figure 8.5).

8.2.2.2 Deposition of polymeric materials

The deposition of the polymers was also confirmed by the same two techniques. For substrates with different coatings, the water dynamic contact angles ranged from 13° for the hydrophilic PAAc to 113° for hydrophobic PDMS for advancing contact angle. The increase or decrease in advancing contact angle of the new layer, when compared with the pure adhesion promoter was due to the hydrophilicity/hydrophobicity of the newly bound polymers.

Regarding the XPS analysis, it is worth noting that our system consists of layers of the adhesion promoter and the polymer. When an overlayer is added to the characterized system, this results in attenuation of the intensity signal from the layers below. Thus, a high signal originating from the substrate and the adhesion promoter layer, represents a thin deposited polymer layer. The more attenuated the signal becomes, the thicker the polymeric layers [45]. Hence, the molecular weight of the polymers constitutes a critical parameter, as higher molecular weight could lead to increased density of polymers, and denser polymer would lead to a thicker coating

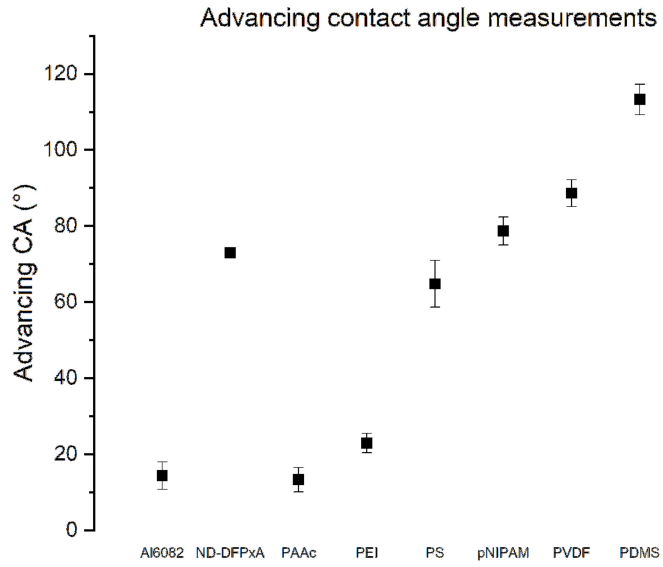

Figure 8.5. Advancing dCA measurements of the freshly cleaned aluminum substrate (Al6082) and of various functionalized surfaces. (Adapted from [77].)

layer that could mask the layers beneath. Thus, depending on the thickness of the coated layer, the composition could be comprised of elements originating from the substrate, the adhesion promoter layer or the top polymeric material. Moreover, according to Serrano *et al* [46], effective attachment of the adhesion promoter differs depending on the polymer used and it appears to be a crucial parameter for the formation of homogeneous coatings.

For PAAc, the substrate signal as well as the signal of the adhesion promoter decreased due to the masking effect of the high molecular weight polyacrylic acid polymer that consists of carbon and oxygen. The composition of the overlayer shows an increase in carbon and a slight increase in oxygen, due to the C=O of the carboxyl bond and it matches with the theoretically calculated one. The measured advancing contact angle was 13°, which agrees with the highly hydrophilic nature of the polymer.

Regarding the chemical composition of PEI, the signals of the substrate and the adhesion promoter were mostly masked by a layer formed from the highly branched polymer that consists of carbon and nitrogen. The main deviation from the theoretical composition was the presence of oxygen in the overlayer, which could be attributed to the aluminum oxides. Hence, a homogeneous PEI film was not successfully achieved.

For pNIPAM, a thin layer was formed from the low molecular weight polymer verified by the high content of C–N and C=O bonds. Again, the presence of fluorine in the composition indicated that the overlayer thickness of pNIPAM was thin and the calculated overlayer composition therefore derived from both layers of adhesion promoter and bound pNIPAM.

For PS, when comparing the chemical composition with the adhesion promoter, one can observe that the presence of an overlayer leads to a decrease of fluorine and

Table 8.1. Surface characterization of the substrate (Al6082 with a naturally grown Al_2O_3 layer), the adhesion promoter layer after activation, and the six investigated polymer films. The samples were characterized by dCA and the apparent normalized atomic concentrations were measured using XPS. In the case of polymer films, the compositions were determined by subtraction of the aluminum and aluminum oxide contributions. Calculated polymer compositions are given in brackets for comparison. (Adapted from [77].)

Chemistry	dCA, Adv/Rec (°)		XPS (normalized At.-%)								
			Mg 1s	Na 1s	Zn 2p3	Al 2p	C 1s	F1s	N 1s	O 1s	Si 2p
Al6082	14 (± 3.6)/14.8 (± 7.2)	At%	9.0	—	—	15.9	19.6	0.5	0.0	53.9	0.4
Adhesion promoter	73 (± 0.8)/17.5 (± 4.4)	At%	1.5	0.0	1.3	12.1	38.5	4.2	6.9	35.4	0.0
		Norm. At%					49.8	5.4	9.0	35.8	0.0
		Theor. At%					(59.4)	(6.2)	(17.2)	(17.2)	(0.0)
PAAc 250 kDa	13 (± 3.2)/5.8 (± 2.7)	At%	0.0	0.0	0.0	12.3	49.5	0.0	0.0	38.2	0.0
		Norm. At%					60.6	0.0	0.0	39.4	0.0
		Theor. At%					(60)	(0.0)	(0.0)	(40)	(0.0)
PEI 25 kDa	23 (± 2.5)/8.8 (± 0.6)	At%	0.0	0.0	0.0	3.2	70.3	0.0	7.5	18.7	0.4
		Norm. At%					73.3	0.0	7.8	18.5	0.4
		Theor. At%					(75)	(0.0)	(25)	(0.0)	(0.0)
PS 280 kDa	65 (± 6.1)/11.9 (± 4.1)	At%	0.5	1.1	2.0	8.1	52.1	2.4	4.8	28.9	0.0
		Norm. At%					61.8	2.9	5.7	29.6	0.0
		Theor. At%					(100.0)	(0.0)	(0.0)	(0.0)	(0.0)
pNIPAM 40 kDa	79 (± 3.7)/16.9 (± 2.3)	At%	1.1	0.0	2.7	14.3	39.7	1.6	4.6	35.9	0.0
		Norm. At%					53.3	2.2	6.2	38.4	0.0
		Theor. At%					(76.2)	(0.0)	(11.9)	(11.9)	(0.0)
PVDF 275 kDa	89 (± 3.6)/35.8 (± 2)	At%	6.7	0.0	1.0	21.3	19.3	4.4	0.0	47.2	0.0
		Norm. At%					35.4	8.2	0.0	56.4	0.0
		Theor. At%					(50.0)	(50.0)	(0.0)	(0.0)	(0.0)
PDMS 330 kDa	113 (± 4)/58.4 (± 3.9)	At%	0.0	0.0	0.0	3.9	51.9	0.9	1.4	25.8	16.3
		Norm. At%					55.2	0.9	1.5	25	17.4
		Theor. At%					(50.0)	(0.0)	(0.0)	(25.0)	(25.0)

an increase in carbon and more specifically in the C–C bond contribution, as expected from the chemical structure of this polymer. The fact that all elements were present in the overlayer suggests that only a rather thin PS film was coated and thus acquisition of signal originating from the substrate, the adhesion promoter and the polymer was possible.

For PVDF, effective coating of the polymer was not achieved, and only partial coating was observed. The overlayer should consist of carbon and fluorine alone. The low fluorine contribution as well as the exceedingly high percentage of Al detected originating from the substrate indicated that PVDF was not successfully attached to form a uniform layer. This is also verified by the dynamic water contact angle measured at 88.5°, which is relatively low compared to the 145° for a uniform PVDF layer [47, 48].

Lastly for PDMS, a reasonably thick layer was deposited masking most of the signal of the substrate. In the composition of the overlayer, small amounts of nitrogen and fluorine were detected due to the adhesion promoter layer as expected from the structure, and the silicon atomic concentration (at%) was increased. At the same time, the contribution of C–C bonds was vastly increased and, in combination with the measured contact angle of 113°, the successful attachment of PDMS was confirmed (figure 8.6).

Successful deposition of the polymers was also confirmed by XPS, except for the case of PVDF and partly PEI. The data revealed that in some cases, the composition originated from all the different layers, suggesting the deposition of quite thin polymeric films. Additionally, interpretation of the content of the different carbon components deriving from the different carbon bonds is essential for definitive determination of successful coating of the polymers (table 8.2). Oxygen concentration showed the greatest deviation across samples which, if higher, is typically attributed to the surface aluminum oxides and hydroxides.

Table 8.2. Normalized C 1s content of different carbon components. The relatively high content of the C=O peak, as observed in most of the chemistries described so far, can be attributed to the presence of the adhesion promoter. (Adapted from [77].)

	Relative peak area (%)			
Chemistry	C–C	C–N, C–O	C–F, C=O	O–C=O
Binding energy	285 ± 0.0 (eV)	286.52 ± 0.09 (eV)	288.75 ± 0.23 (eV)	289.85 ± 0.0 (eV)
Al6082	68.3	9.0	—	22.7
Adhesion promoter	53.9	37.4	8.6	—
PAAc 250 kDa	55.9	17.6	17.6	9.0
PEI 25 kDa	67.5	20.1	12.4	—
PS 280 kDa	65.7	24.4	10.0	—
pNIPAM 40 kDa	56.8	31.2	12.0	—
PVDF 275 kDa	63.2	21.5	15.3	—
PDMS 330 kDa	78.5	14.1	7.3	—

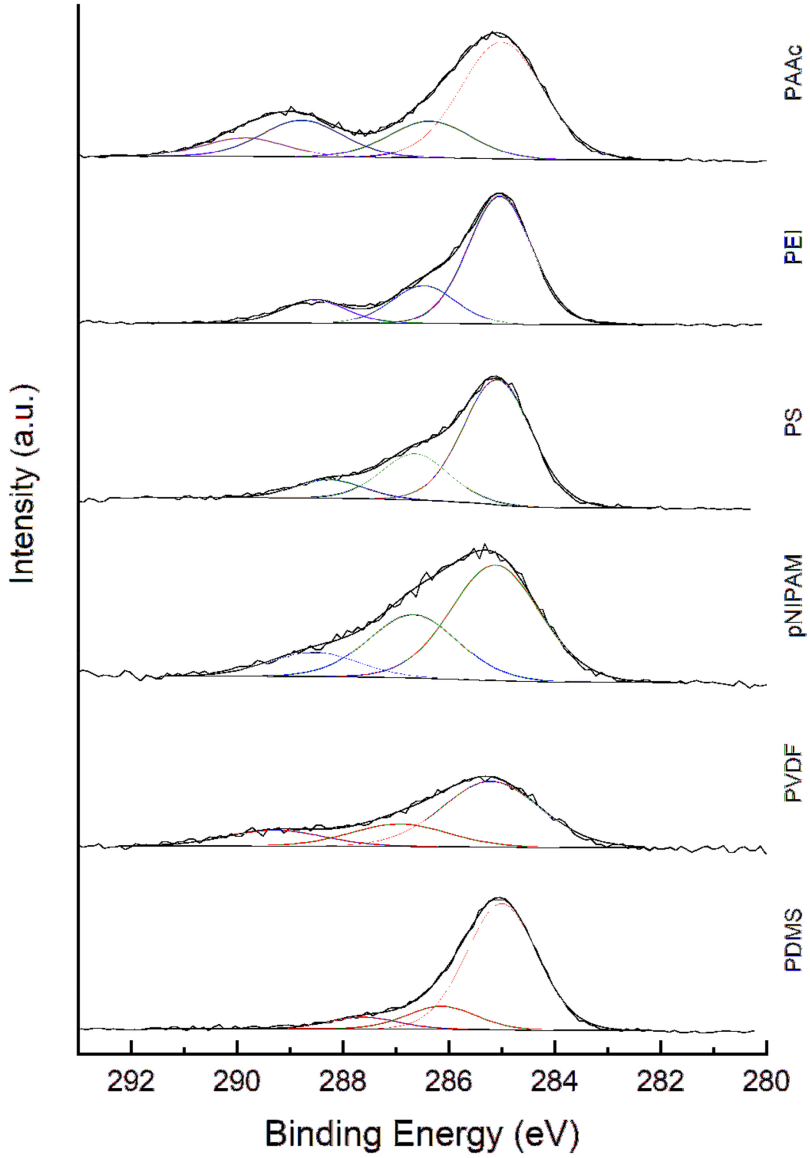

Figure 8.6. Detailed XPS spectra of the C 1s region on the bare Al6082 and various functionalized surfaces. Curve-fitted carbon component C–C, in red; C–N, C–O in green; C–F, C=O in blue; and O–C=O in purple. (Adapted from [77].)

8.2.2.3 Ice adhesion strength correlates with the surface wettability

When ice forms on surfaces with features that allow it to lodge firmly as on hydrophilic surfaces, the water molecules at the interface between the surface and the ice tend to align in a way that maximizes hydrogen bonding interactions, leading to mechanical interlocking [49]. Therefore, hydrophilic surfaces present higher ice adhesion compared to hydrophobic ones, where fewer hydrogen bonds are present [50].

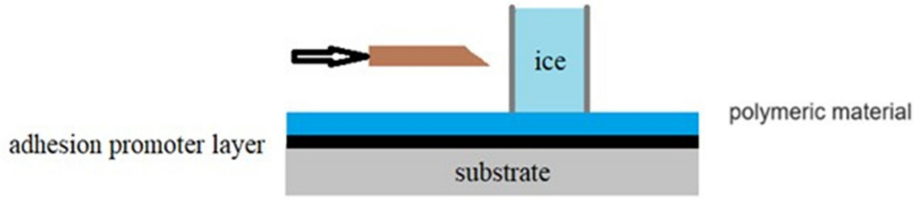

Figure 8.7. Graphical representation of ice adhesion measurements on a standard sample. (Adapted from [77].)

The force–time curves showed a sharp detachment of the ice block for all samples, indicating a behavior of rigid-like materials. Even the PDMS sample showed a sharp detachment, indicating variation between monolayer thick PDMS coating and bulk PDMS, which behave as an elastic material that in combination with the high hydrophobicity yields low strength values of ice adhesion [51]. The force data measured were used to calculate the adhesion strength by dividing the values with the surface area of the formed ice block (figure 8.7).

Two sets of experiments were performed with different diameters of ice block formation, to assess the impact of the ice–substrate interface on the adhesion strength. The first approach was to investigate the detachment of an ice block with diameter of 8 mm [26].

Most of the measurements on the hydrophilic samples—Al6082, PAAc and PEI—exhibited adhesion strength values that are out of range, since the maximum force value (110 N) that the sensor could measure was reached and thus acquisition of the force value in some instances was not achieved. As the surface wettability decreased (increasing contact angles) the adhesion strength of the ice decreased, suggesting a correlation between ice adhesion strength and surface wettability (figure 8.8).

Since the acquisition of force values on most of the hydrophilic samples was not achieved, we also decided to investigate the ice adhesion strength using an ice block with a smaller diameter of 5.4 mm wide.

In this case, force values of the ice detachment were acquired in all measurements, apart from for the PAAc samples. The data demonstrate the same pattern as the previous data set, where high ice adhesion strength was associated with the most hydrophilic samples and decreased upon increasing hydrophobicity of the sample (figure 8.8). Overall, although ice adhesion strength values were acquired, the trend is confirmed principally for the hydrophobic coatings and our data set was mostly dominated by hydrophilic samples. Therefore, more measurements with wider wettability surface ranges are necessary to better understand the key correlation.

Furthermore, all values of ice adhesion strength were much higher than 100 kPa, a fact that could be attributed to the thickness of the deposited polymers, which is in the range of a few nanometers, and they behave like rigid materials showing a sharp detachment of ice. Thus, they present increased stiffness compared to soft elastomeric coatings known to lead to lower ice adhesion strength due to their lower intrinsic surface energy and higher flexibility [28, 52].

Moreover, according to Gao and McCarthy [53], the wettability (or repellency) of a substrate from a thermodynamic viewpoint can be associated with the formation

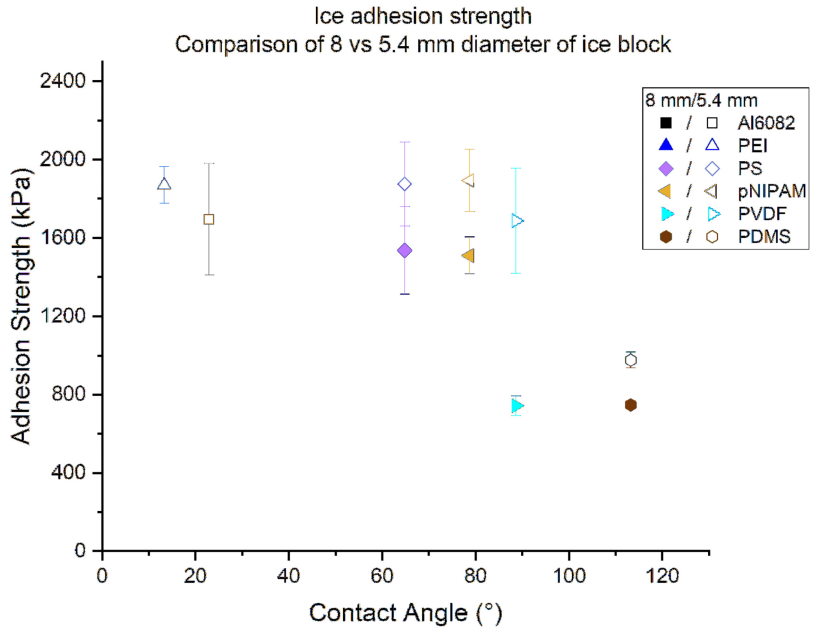

Figure 8.8. Ice adhesion strength values of the different polymeric coated samples. Comparison of ice block diameters of 8 mm versus 5.4 mm. The adhesion strength values of the Al6082, PEI and PAAc samples with an 8 mm ice block and PAAc samples with a 5.4 mm ice block were not determined, since the maximum measurable force value from the sensor was reached. (Adapted from [77].)

and elimination of interfacial areas. Thus, the forces required to separate surfaces connected by a capillary bridge of water are governed by the receding contact angle θ_{rec}. Meuler *et al* [29] observed a strong correlation between the measurements of the average strength of ice adhesion and the practical work of adhesion scaling parameter $[1 + \cos\theta_{rec}]$ for liquid water, suggesting that the 'icephobicity' of nominally smooth surfaces can be predicted simply by measuring the receding contact angle for water droplets on the substrate. They also suggested that the average strength of ice adhesion should follow a linear line which approaches zero, and consequently their data were fitted with the constraint that the linear correlations pass through the origin.

For this specific data set by extrapolating for the best linear fitting of figure 8.9 ($R^2 = 0.92$), the expected receding contact angle of an icephobic polymeric monolayer coating (ice adhesion strength <100 kN) according to our findings, would be a receding angle of 83° or more.

Our data are mostly dominated by hydrophilic samples and only the hydrophobic PDMS point deviates substantially. Moreover, they are located in a completely different region both of ice adhesion strength values, and receding contact angles as well. Thus, direct comparison with previous findings from Meuler *et al* is not possible.

A factor behind this variation could be the difference in the roughness of the substrate material, which was measured to be approximately 0.5 μm, and lower in all cases compared to Meuler *et al*. This difference in the roughness may influence

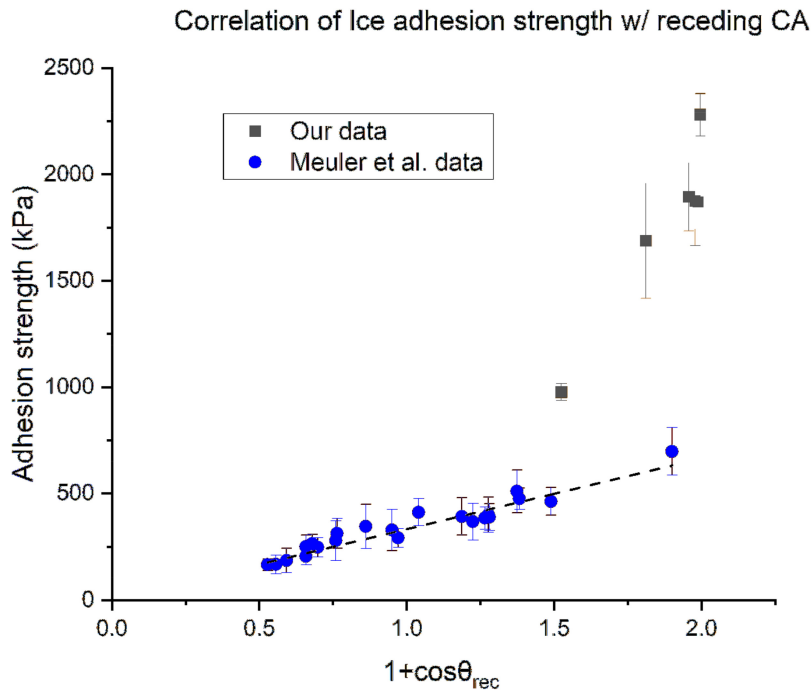

Figure 8.9. Ice adhesion strength values against $[1 + \cos\theta_{rec}]$. Our data are compared to data from Meuler *et al* [29]. (Adapted from [77].)

the surface topography, providing sites for water retention and ice nucleation, leading to lower measured receding contact angles and to increased interlocking of ice [54–56]. Also, Mostofi Sarkari *et al* [57] have shown that previous correlations based on the receding contact angle have produced contradictory results. Nevertheless, most of the samples present low receding angles and only a few hydrophobic samples were measured, resulting in an uneven distribution of data points. Thus, this validates that further investigation of the surface topography and the underlying mechanisms is essential.

8.2.3 Conclusion

In this study, we proved that the use of an adhesion promoter layer containing the DFPxA moiety provides a versatile approach for the functionalization of aluminum surfaces with a variety of polymers in a reliable manner. We have used this approach to test the binding capability of the adhesion promoter with multiple polymers that span different wetting properties. The adhesion promoter possesses the ability to coordinatively bind to aluminum surfaces through nitro-catechol end groups and, upon activation, covalently bond to polymers in its close proximity through the reactive nitrene groups, which undergo insertion reaction to any C–H, C–C, or C–N bonds. Validation of the polymer deposition was achieved by means of different surface characterization techniques, such as dynamic contact angle and XPS. Moreover, regarding the behavior of the functionalized polymeric monolayers for

ice detachment, they demonstrated a rigid-like material behavior resulting in sharp detachment of the ice block. For that, a horizontal shear (or push) test was used to acquire the force values, and the analysis of the data revealed a correlation between increased ice adhesion strength values and high surface wettability, whereas samples with high contact angles exhibited lower values of adhesion strength, in agreement with previous studies.

8.3 Ultrathin adhesion promoter films for gluing and bonding applications

8.3.1 Introduction

In the field of surface engineering, polymeric coatings constitute a primary approach to modify surfaces to introduce desired functionalities without compromising the properties of the underlying bulk material [58]. Adhesion strength is a crucial property in coatings as it significantly influences the durability and performance of the coating system. Moreover, it is a critical factor in determining the efficacy and longevity of coatings, as it ensures that the coating remains attached even under stress in harsh operating conditions, reducing the need for frequent reapplications or repairs [59, 60]. Understanding the factors that influence adhesion strength, such as substrate and coating composition, or innovative coating techniques are therefore essential for the development of robust and high-performance coating systems [61].

Mechanical characterization of the adhesion strength is performed with the commonly used lap shear tests to evaluate the effect of an adhesion promoter [62, 63]. These tests are essential for quantifying adhesion strength via the acquisition of the shear force necessary to separate the bound materials and for evaluating the performance of different adhesive systems. The outcomes offer valuable insights into the bonding ability of adhesives, facilitating the design of adhesive materials with improved adhesion properties for a variety of applications. The lap shear adhesion strength is influenced by various factors, such as the type of adhesive used, the presence of cross-linkers, and the curing process [64, 65].

In this work, we immobilized polymers on different types of substrates with the use of an adhesion promoter for assessing their adhesion strength. For that, lap shear tests were used to assess the adhesive bond strength of bound samples, using cyclic olefin copolymers (COCs) or epoxy as adhesives. The use of an adhesion promoter layer, capable of forming covalent bonds with any neighboring C–C bond via nitrene insertion, increased the adhesion strength of the adhesives up to four times compared to samples without an adhesion promoter, improving their mechanical durability, therefore creating an appropriate coating platform for adhesives that would not bind otherwise. Thermal curing of the samples results in simultaneous activation of the adhesion promoter to covalently bond with the adhesive, while curing of the adhesive occurred.

8.3.2 Results and discussion

An adhesion promoter layer can increase the adhesion strength of bound systems. To evaluate the adhesion strength of bound specimens containing an adhesion

promoter layer, measurements of the force necessary to separate them under shear loading were performed according to the widely used single lap shear test [66] (figure 8.10).

Aluminum alloy 5005 (Al5005), glass fiber (GF) reinforced with epoxy, and polypropylene (PP) specimens were used as substrate materials. Aluminum was chosen as a relevant material for aerospace applications, since the parts on airplane wings requiring anti-icing surfaces are made of this material [67]. Polymeric materials and glass fiber reinforced polymers were chosen as relevant materials for multiple industrial applications [68, 69]. Regarding the adhesion promoters used, the DFPxA and PFPA reactive moieties were functionalized by additional end groups for them to attach to the different substrates. More specifically, for attachment to the Al5005 substrate, DFPxA and PFPA reactive moieties were functionalized with a nitrodopamine catechol (ND-DFPxA and ND-PFPA) known to strongly bind to aluminum (figure 8.2(a)). In the case of attachment to the PP and GF substrates, the reactive moieties were grafted to the branched PEI containing amine groups. The PEI-g-DFPxA and PEI-g-PFPA adhesion promoters bind electrostatically to glass and plasma treated polymers and/or covalently to any nearby carbon atom from the

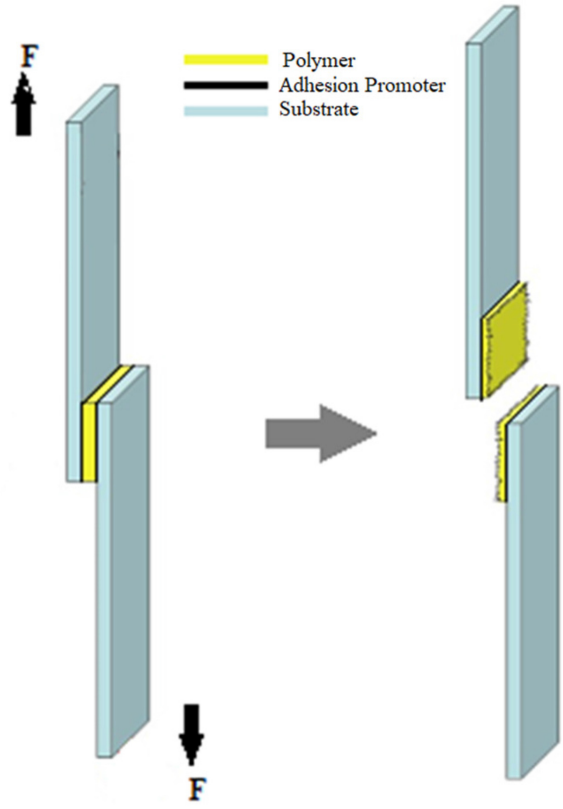

Figure 8.10. The prepared bound samples were tested by the single lap shear test, where the force necessary to separate the two specimens is measured. (Adapted from [77].)

substrate, the coating or within the adhesion promoting layer, after activation of the azides (figure 8.2(b)). Finally, the top coatings/adhesives used were COCs, a material where no adhesive strength is expected due to its inertness and lack of functionality, and a low temperature one-component epoxy as a commercial high strength adhesive. These materials were chosen to physico-chemically represent industry-relevant functionalities, such as high transparency, high thermal stability, hydrophobicity, chemical resistance, a barrier to oxygen and water vapor, and durability [70–72].

To prepare the samples, two identical pieces coated with an adhesion promoter layer containing a reactive aryl azide and the desired adhesive (COC or epoxy) were prepared separately (figure 8.11). Solvent bonding at an elevated temperature of the two pieces was performed by addition of two droplets of the coating material. The overlapping area of the two pieces was 12.5 mm in length and 25 mm in width and they were finally gripped with a screw clamp. The resulting specimens were cured at 80 °C in an oven for 2 h to activate the azides, leading to the formation of covalent bonds with the polymeric topcoat. Control samples that were not coated with an adhesion promoter layer were prepared and measured for comparison.

With the designed experiments, the increase of adhesion strength of the newly synthesized adhesion promoters containing the DFPxA reactive moiety with an activation temperature ~80 °C was quantified and compared with samples containing adhesion promoters with the PFPA moiety. The latter are well established adhesion promoters known to become activated when exposed to temperatures higher than 120 °C. Consequently, PFPA-containing adhesion promoters were not expected to be activated at 80 °C, the temperature to which the samples were exposed, in contrast to the recently developed DFPxA containing adhesion promoters. At the same time, control samples containing no adhesion promoter but only COC or epoxy were prepared and cured using the same conditions.

When COC was used as an adhesive polymer, the adhesion strength was highest for the samples containing DFPxA adhesion promoters, which suggests that they were successfully attached both to the substrate and the top-coating of COC after activation. The measured strength values exhibited an almost 100% increase in strength when used for the Al5005 and PP substrates, and in the case of glass fiber we observed a four times increase in adhesion. For PP and Al5005, the data suggest that

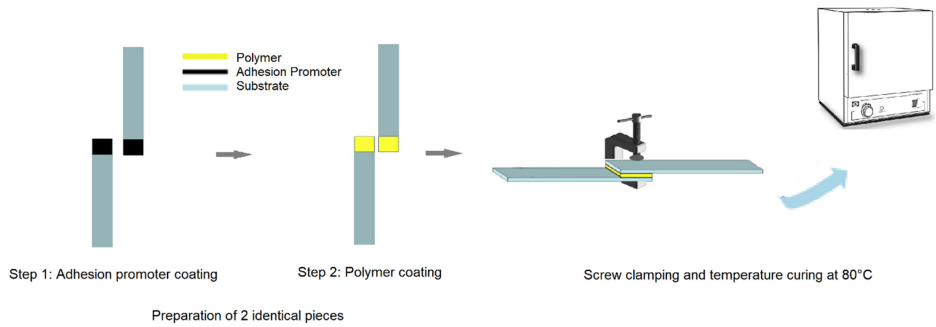

Figure 8.11. Preparation of bound samples for lap shear tests. (Adapted from [77].)

even the use of the PFPA-containing adhesion promoters, expected not to be activated at 80 °C, slightly increased the adhesion strength of the samples, presumably since they provides a more suitable platform for the coating of COC on the substrate (figure 8.12).

In the next experiment, a low temperature curing 'one-component' epoxy was used. It provides unlimited working time at room temperature, but most importantly it can be cured simultaneously with the adhesion promoter's activation. Using such an adhesive in between the two bound specimens, the values of adhesion strength were significantly higher compared to COC, since the cured epoxy is a very strong material. The epoxy adhered well to bare Al5005, and the use of a non-activated adhesion promoter (ND-PFPA) did not confer additional substantial benefit. For the activated ND-DFPxA adhesion promoter, the adhesion strength of the system was increased slightly, suggesting that formation of covalent bonds with epoxy increased its strength, nevertheless adhesion was already suitable.

The adhesion using the glass fiber reinforced epoxy substrate was quite different. Samples without adhesion promoter resulted in the highest adhesion strength of the whole series, since the substrate already contains an epoxy material and the affinity between the substrate and epoxy adhesive was extensive. The application of an adhesion promoting layer led to a decrease of the adhesion strength, since the epoxy was not directly coated on the glass fiber substrate and the affinity is lower. Nonetheless, the use of the activated PEI-g-DFPxA doubled the adhesion strength compared to PEI-g-PFPA, suggesting the formation of covalent bonds with the epoxy glue.

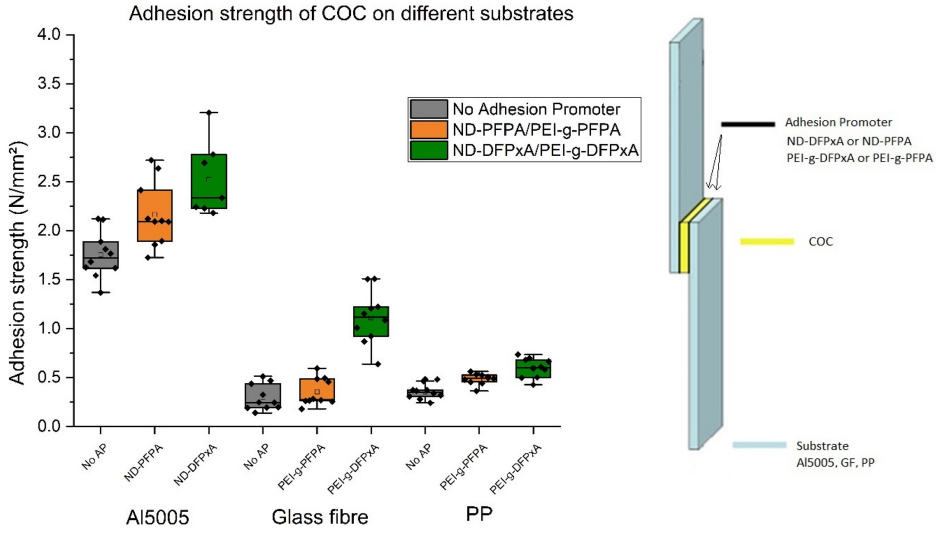

Figure 8.12. Comparison of the adhesion strength between all the substrates and conditions when COC was used as an adhesive. The gray boxplots correspond to the samples without any adhesion promoter layer, the orange to the samples with adhesion promoters containing the PFPA moiety which were expected not to be activated at the curing temperature of 80 °C and lastly the green boxplots correspond to the samples with adhesion promoters containing the DFPxA moiety which were expected to be activated at 80 °C and covalently attach to the COC. (Adapted from [77].)

Lastly, the outcome of the tests with PP specimens is very straightforward. It is well known that epoxy adhesives do not work well with non-polar polymeric materials since their affinity is low [73, 74], as validated from the very low adhesion strength of the control samples without adhesion promoter. The use of both adhesion promoters created an appropriate coating platform for epoxy, and acquisition of the force values for the assessment of the adhesion strength was not possible, since failure of the PP substrate itself occurs. It is evident, however, that the use of an adhesion promoter increased vastly the capability of an epoxy to be coated on polypropylene, materials that do not have affinity with each other (figure 8.13). That the epoxy can react with amino groups of the adhesion promoter was expected, nevertheless, this is an unexpected finding since it was not anticipated that the non-activated PEI-g-PFPA would bind so strongly on the PP substrate.

After the outcome of the above performed experiments, we demonstrated that we could immobilize numerous polymeric coatings with the use of a thermally activated, nanoscale thick adhesion promoter layer, increasing their adhesion strength. As a next step, we considered bonding two specimens together without deformation or degradation, just by using an adhesion promoter layer. For that reason, polymethyl methacrylate (PMMA) specimens were chosen as a polymer demonstrating a low glass transition temperature, of approximately 105 °C, that is non UV-C transparent as well [75]. Thus, the only possible way to bond such materials is using a low temperature activated adhesion promoter such as PEI-g-DFPxA.

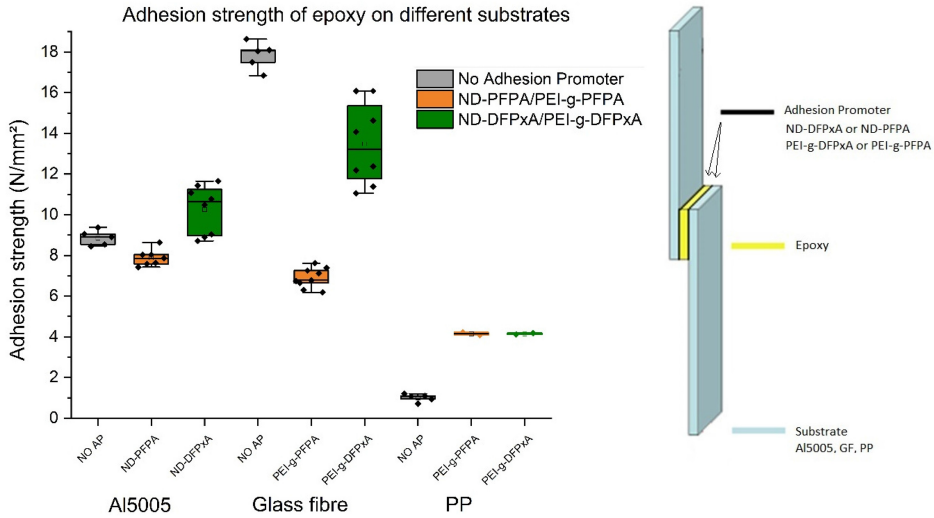

Figure 8.13. Comparison of adhesion strength between all substrates and conditions when low temperature curing epoxy was used as the adhesive. The gray boxplots correspond to the samples without any adhesion promoter layer, the orange to the samples with adhesion promoters containing the PFPA moiety which were expected not to be activated at the curing temperature of 80 °C and lastly the green boxplots correspond to the samples with adhesion promoters containing the DFPxA moiety which were expected to be activated at 80 °C and covalently attach to the epoxy. The adhesion strengths of PP in the cases of PEI-g-PFPA and PEI-g-DFPxA at approximately 4.2 N mm^{-2} do not correspond to failure of the epoxy rather than failure of the PP substrate material. (Adapted from [77].)

The bonding of two PMMA specimens at a temperature higher than its glass transition led to deformation and rearrangement of the PMMA macromolecular chains which entangled upon transition back to brittle behavior [76], represented as high measured adhesion force. This finding validated the need for a system that is activated at temperatures below 100 °C, and thus the temperature chosen to test the effect of the adhesion promoters was 90 °C. It is clear that the adhesion force after curing is the highest when the activated PEI-g-DFPxA was used for bonding (figure 8.14).

These preliminary results show that this idea is promising, and that PEI-g-DFPxA can be used to bond materials at temperatures below 100 °C. Nevertheless, there are some factors that need to be considered, such as the difficulty presented

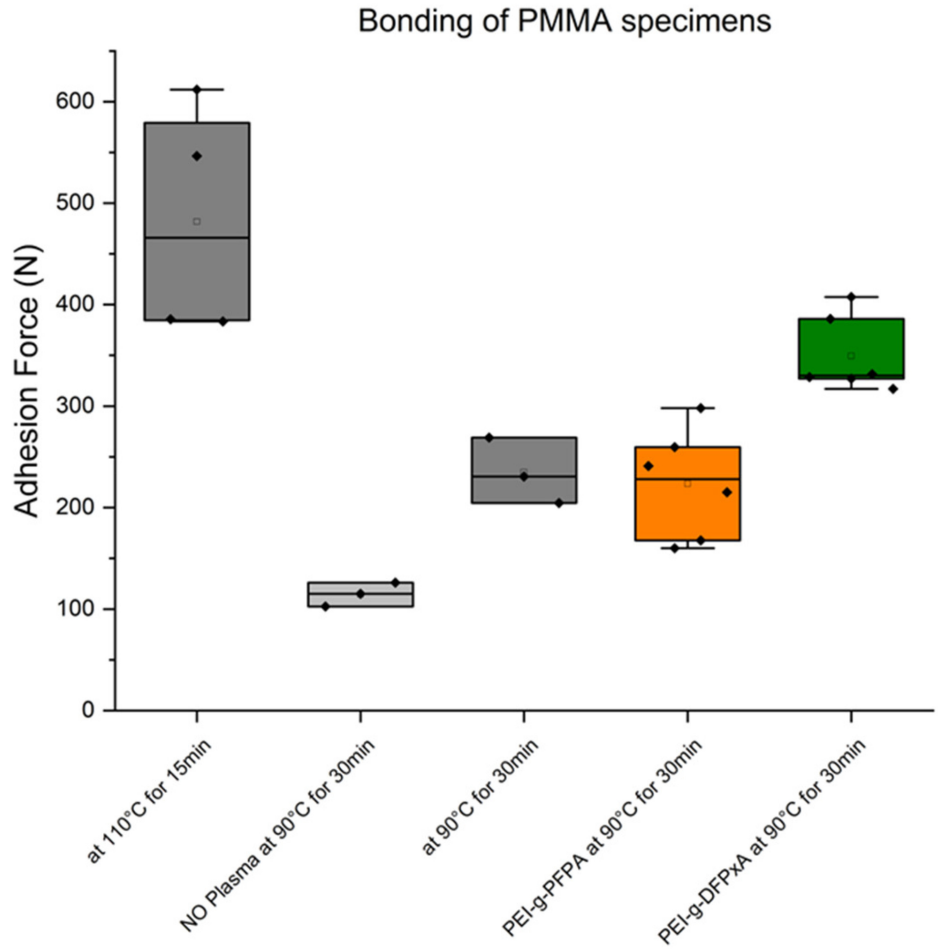

Figure 8.14. Force adhesion measurements of thermally bonded PMMA sheets with and without the use of adhesion promoters. PMMA exhibits a glass transition temperature at approximately 105 °C, thus it shows high adhesion force due to deformation and rearrangement of the PMMA chains. At 90 °C no deformation occurs and the activated PEI-g-DFPxA results in the higher adhesion force at this temperature. (Adapted from [77].)

when trying to bond substrates which are not perfectly flat, rather having a microscale structure, with a nanometer thick adhesion promoter layer. Investigation of the optimal parameters and conditions is still ongoing.

8.3.3 Conclusion

Here, we demonstrated that an engineered adhesion promoter can create an appropriate coating platform for the application of coatings and increase the adhesion strength of the system after activation and formation of covalent bonds with the adhesive. The adhesion strength of samples containing an adhesive (such as COC and epoxy), using different activated or not activated adhesion promoters, on three different substrates (Al5005, glass fiber and PP) was investigated by performing lap shear measurements. It was demonstrated that intrinsically purely adhered materials can be covalently coated, and improved durability of coatings under mechanical stresses can be achieved with the use of an activated adhesion promoter. Thermal activation of the samples in the experimental set-up resulted in simultaneous activation of the azides to covalently bind with the adhesive, while curing of the adhesive occurring. The adhesion promoters containing the reactive DFPxA moiety, which is demonstrated to be activated already at 70 °C, can improve the adhesion between Al or glass fiber substrates and a non-activated polymer such as COC. Moreover, they constitute promising materials for increasing adhesion between non-polar polymeric substrates such as PP and epoxy at low temperatures.

8.4 Results overview

DFPxA-based adhesion promoters that are activatable at the lowest temperature were investigated for their binding capability with different polymer materials but also for their effect on the adhesion strength of a coating system. Our findings indicate that the thermally activated adhesion promoter can non-specifically insert to polymers that do not carry functional end groups via the formation of covalent bonds, leading to their permanent immobilization on different substrates. Thus, we successfully surface-tethered monolayers of different polymers with diverse surface wettability, and by measuring the adhesion strength of a formed ice block on top, we correlated the high surface wettability with decreased ice adhesion strength values. Moreover, it was demonstrated that bound samples containing an activated adhesion promoter and an adhesive polymer can lead to an increase of adhesion strength by up to four times when cured at low temperatures of ~80 °C, compared to non-activated samples.

References

[1] Li F *et al* 2018 Advanced composite 2D energy materials by simultaneous anodic and cathodic exfoliation *Adv. Energy Mater.* **8** 1–8

[2] Zhao X, Cai Y, Wang T, Shi Y and Jiang G 2008 Preparation of alkanethiolate-functionalized core/shell Fe_3O_4@Au nanoparticles and its interaction with several typical target molecules *Anal. Chem.* **80** 9091–6

[3] Quan Z *et al* 2015 Additive manufacturing of multi-directional preforms for composites: opportunities and challenges *Mater. Today* **18** 503–12
[4] Granozzi G 2023 Impact of surface science in current science and technology: some basic considerations *Surfaces* **6** 533–5
[5] Alaei Shahmirzadi M A and Kargari A 2018 *Nanocomposite Membranes* (Amsterdam: Elsevier)
[6] Li C J 2010 Thermal spraying of light alloys *Surface Engineering of Light Alloys: Aluminium, Magnesium and Titanium Alloys* (Woodhead: Cambridge) pp 184–241
[7] Vieira T, Castanho J and Louro C 2006 Hard coatings based on metal nitrides, metal carbides and nanocomposite materials. PVD process and properties *Materials Surface Processing by Directed Energy Techniques* (Amsterdam: Elsevier) pp 537–72
[8] Camperi J, Pichon V and Delaunay N 2020 Separation methods hyphenated to mass spectrometry for the characterization of the protein glycosylation at the intact level *J. Pharm. Biomed. Anal.* **178** 112921
[9] Konai M M, Bhattacharjee B, Ghosh S and Haldar J 2018 Recent progress in polymer research to tackle infections and antimicrobial resistance *Biomacromolecules* **19** 1888–917
[10] Zhou G and Groth T 2018 Host responses to biomaterials and anti-inflammatory design—a brief review *Macromol. Biosci.* **18** 1–15
[11] Michelmore A 2016 *Thin Film Growth on Biomaterial Surfaces* (Amsterdam: Elsevier)
[12] Hale A, Macosko C W and Bair H E 1991 Glass transition temperature as a function of conversion in thermosetting polymers *Macromolecules* **24** 2610–21
[13] Lindholm E A, Stolov A A, Dyer R S, Slyman B and Burgess D 2009 Reliability of optical fibers in a cryogenic environment *Fiber Optic Sens. Appl. VI* **7316** 73160Z
[14] Eßbach C, Fischer D and Nickel D 2021 Challenges in electroplating of additive manufactured ABS plastics *J. Manuf. Process.* **68** 1378–86
[15] Sastri V R 2010 Commodity thermoplastics *Plastics in Medical Devices* (Amsterdam: Elsevier) pp 73–119
[16] Samavedi S, Poindexter L K, Van Dyke M and Goldstein A S 2014 *Synthetic Biomaterials for Regenerative Medicine Applications* (Amsterdam: Elsevier)
[17] Hasan A and Pandey L M 2015 Review: polymers, surface-modified polymers, and self assembled monolayers as surface-modifying agents for biomaterials *Polym. Plast. Technol. Eng.* **54** 1358–78
[18] Ratner B D 1995 Surface modification of polymers: chemical, biological and surface analytical challenges *Biosens. Bioelectron.* **10** 797–804
[19] Brannon H 2014 The development of novel adhesion promoters for waterborne coatings and polypropylene car bumpers *PhD Thesis* University of Birmingham
[20] Kost J, Bleiziffer A, Rusitov D and Rühe J 2021 Thermally induced cross-linking of polymers via C,H insertion cross-linking (CHic) under mild conditions *J. Am. Chem. Soc.* **143** 10108–19
[21] Abu Bakar R, Li Y, Hewitson O P, Roth P J and Keddie J L 2022 Azide photochemistry in acrylic copolymers for ultraviolet cross-linkable pressure-sensitive adhesives: optimization, debonding-on-demand, and chemical modification *ACS Appl. Mater. Interfaces* **14** 30216–27
[22] Atzemoglou A A, Bartalucci N, Donat F, Tibbitt M W, Tosatti S G P and Zürcher S 2025 Development of low temperature activatable aryl-azide adhesion promoters for versatile surface modifiers *ACS Appl. Eng. Mater.* **3** 867–82

[23] Civil Aviation Authority 2000 *Aircraft Icing Handbook* (New Zealand: Safety Education and Publishing Unit) pp 1–20
[24] Lynch F T and Khodadoust A 2001 Effects of ice accretions on aircraft aerodynamics *Prog. Aerosp. Sci.* **37** 669–767
[25] Laforte J L, Allaire M A and Laflamme J 1998 State-of-the-art on power line de-icing *Atmos. Res.* **46** 143–58
[26] Stendardo L *et al* 2023 Reframing ice adhesion mechanisms on a solid surface *Appl. Surf. Sci.* **641** 158462
[27] PRO-ACT 1998 Air force aircraft and airfield deicing/anti-icing the role of deicing and anti-icing in the air force types of deicing and anti-icing agents *Fact Sheet* TI-16621 PRO-ACT 1–7
[28] Wang C, Fuller T, Zhang W and Wynne K J 2014 Thickness dependence of ice removal stress for a polydimethylsiloxane nanocomposite: Sylgard 184 *Langmuir* **30** 12819–26
[29] Meuler A J, Smith J D, Varanasi K K, Mabry J M, McKinley G H and Cohen R E 2010 Relationships between water wettability and ice adhesion *ACS Appl. Mater. Interfaces* **2** 3100–10
[30] Yang S, Xia Q, Zhu L, Xue J, Wang Q and Chen Q M 2011 Research on the icephobic properties of fluoropolymer-based materials *Appl. Surf. Sci.* **257** 4956–62
[31] Golovin K, Kobaku S P R, Lee D H, DiLoreto E T, Mabry J M and Tuteja A 2016 Designing durable icephobic surfaces *Sci. Adv.* **2** e1501496
[32] Jellinek H H G 1962 Ice adhesion *Can. J. Phys.* **40** 1294–309
[33] Marengo M 2022 *The Surface Wettability Effect on Phase Change* (Cham: Springer)
[34] Shen Y, Wu X, Tao J, Zhu C, Lai Y and Chen Z 2019 Icephobic materials: fundamentals, performance evaluation, and applications *Prog. Mater Sci.* **103** 509–57
[35] Huang J, Lou C, Xu D, Lu X, Xin Z and Zhou C 2019 Cardanol-based polybenzoxazine superhydrophobic coating with improved corrosion resistance on mild steel *Prog. Org. Coat.* **136** 105191
[36] Yeong Y H, Milionis A, Loth E, Sokhey J and Lambourne A 2015 Atmospheric ice adhesion on water-repellent coatings: wetting and surface topology effects *Langmuir* **31** 13107–16
[37] Subramanyam S B, Rykaczewski K and Varanasi K K 2013 Ice adhesion on lubricant-impregnated textured surfaces *Langmuir* **29** 13414–8
[38] Kulinich S A and Farzaneh M 2009 How wetting hysteresis influences ice adhesion strength on superhydrophobic surfaces *Langmuir* **25** 8854–6
[39] He Z, Vågenes E T, Delabahan C, He J and Zhang Z 2017 Room temperature characteristics of polymer-based low ice adhesion surfaces *Sci. Rep.* **7** 1–7
[40] Sever M J, Weisser J T, Monahan J, Srinivasan S and Wilker J J 2004 Metal-mediated cross-linking in the generation of a marine-mussel adhesive *Angew. Chem. Int. Ed.* **43** 448–50
[41] Malisova B, Tosatti S, Textor M, Gademann K and Zürcher S 2010 Poly(ethylene glycol) adlayers immobilized to metal oxide substrates through catechol derivatives: influence of assembly conditions on formation and stability *Langmuir* **26** 4018–26
[42] Krishna D N G and Philip J 2022 Review on surface-characterization applications of x-ray photoelectron spectroscopy (XPS): recent developments and challenges *Appl. Surf. Sci. Adv.* **12** 100332
[43] Singh P, Singh R K and Das A K 2024 Optimization of heat treatment cycle for cast-Al6082 alloy to enhance the mechanical properties *Eng. Res. Express* **6** 015036
[44] Greenwood N N and Earnshaw A 1984 *Chemistry of Elements* 2nd edn (Butterworth Heinemann) ch 7 pp 216–67

[45] Tosatti S, Michel R, Textor M and Spencer N D 2002 Self-assembled monolayers of dodecyl and hydroxy-dodecyl phosphates on both smooth and rough titanium and titanium oxide surfaces *Langmuir* **18** 3537–48
[46] Serrano Â *et al* 2013 Nonfouling response of hydrophilic uncharged polymers *Adv. Funct. Mater.* **23** 5706–18
[47] Kamaz M, Sengupta A, Gutierrez A, Chiao Y H and Wickramasinghe R 2019 Surface modification of PVDF membranes for treating produced waters by direct contact membrane distillation *Int. J. Environ. Res. Public Health* **16** 685
[48] Gontarek-Castro E, Rybarczyk M K, Castro-Muñoz R, Morales-Jiménez M, Barragán-Huerta B and Lieder M 2021 Characterization of PVDF/graphene nanocomposite membranes for water desalination with enhanced antifungal activity *Water* **13** 1279
[49] Ling E J Y, Uong V, Renault-Crispo J S, Kietzig A M and Servio P 2016 Reducing ice adhesion on nonsmooth metallic surfaces: wettability and topography effects *ACS Appl. Mater. Interfaces* **8** 8789–800
[50] Emelyanenko K A, Emelyanenko A M and Boinovich L B 2020 Water and ice adhesion to solid surfaces: common and specific, the impact of temperature and surface wettability *Coatings* **10** 1–23
[51] Ibáñez-Ibáñez P F, Montes Ruiz-Cabello F J, Cabrerizo-Vílchez M A and Rodríguez-Valverde M A 2022 Ice adhesion of PDMS surfaces with balanced elastic and water-repellent properties *J. Colloid Interface Sci.* **608** 792–9
[52] Fu Q *et al* 2014 Development of sol gel icephobic coatings: effect of surface roughness and surface free energy *Thin Films 2014. The 7th Int. Conf. on Technological Advances of Thin Films and Surface Coatings*
[53] Gao L and Mccarthy T J 2008 Teflon is hydrophilic. Comments on definitions of hydrophobic, shear versus tensile hydrophobicity, and wettability characterization *Langmuir* **24** 546–50
[54] Wang X and Zhang Q 2020 Role of surface roughness in the wettability, surface energy and flotation kinetics of calcite *Powder Technol.* **371** 55–63
[55] Wang J, Wang S and Hou X 2024 Study on the dependence between surface topography and icephobic behavior of Ni–Cu–P ternary coatings *Adv. Eng. Mater.* **26** 1–10
[56] Cui W, Jiang Y, Mielonen K and Pakkanen T A 2019 The verification of icephobic performance on biomimetic superhydrophobic surfaces and the effect of wettability and surface energy *Appl. Surf. Sci.* **466** 503–14
[57] Mostofi Sarkari N *et al* 2025 Experimental debate on the overlooked fundamental concepts in surface wetting and topography vs ice adhesion strength relationships *J. Colloid Interface Sci.* **682** 825–48
[58] Pruchniewski M *et al* 2023 Nanostructured graphene oxide enriched with metallic nanoparticles as a biointerface to enhance cell adhesion through mechanosensory modifications *Nanoscale* **15** 18639–59
[59] Vengadaesvaran B, Rau S R, Ramesh K, Puteh R and Arof A K 2010 Preparation and characterisation of phenyl silicone-acrylic polyol coatings *Pigm. Resin Technol.* **39** 283–7
[60] Díaz Téllez J P, Harirchian-Saei S, Li Y and Menon C 2013 Adhesion enhancement of biomimetic dry adhesives by nanoparticle *in situ* synthesis *Smart Mater. Struct.* **22** 105031
[61] Nedela O, Slepicka P and Švorcík V 2017 Surface modification of polymer substrates for biomedical applications *Materials* **10** 1115

[62] Gomez-Lopez A, Grignard B, Calvo I, Detrembleur C and Sardon H 2022 Accelerating the curing of hybrid poly(hydroxy urethane)-epoxy adhesives by the thiol-epoxy chemistry *ACS Appl. Polym. Mater.* **4** 8786–94
[63] Zong H, Fang C, Lin Z, Yan Q and Lin X 2020 A novel polyether polyol contains repeating cyclohexane units and its application on reactive polyurethane adhesive *Polym. Adv. Technol.* **31** 2535–44
[64] Samanta S, Banerjee S L, Bhattacharya K and Singha N K 2021 Graphene quantum dots-ornamented waterborne epoxy-based fluorescent adhesive via reversible addition-fragmentation chain transfer-mediated miniemulsion polymerization: a potential material for art conservation *ACS Appl. Mater. Interfaces* **13** 36307–19
[65] Zhou J *et al* 2015 Adhesion properties of catechol-based biodegradable amino acid-based poly(ester urea) copolymers inspired from mussel proteins *Biomacromolecules* **16** 266–74
[66] Abdolah Zadeh M, Van Der Zwaag S and Garcia S J 2016 Adhesion and long-term barrier restoration of intrinsic self-healing hybrid sol–gel coatings *ACS Appl. Mater. Interfaces* **8** 4126–36
[67] Xia A *et al* 2022 Fabrication of an anti-icing aluminum alloy surface by combining wet etching and laser machining *Appl. Sci.* **12** 2119
[68] Wang R *et al* 2021 Mass-synthesized solution-processable polyimide gate dielectrics for electrically stable operating OFETs and integrated circuits *Polymers* **13** 3715
[69] Han M J and Khang D Y 2015 Glass and plastics platforms for foldable electronics and displays *Adv. Mater.* **27** 4969–74
[70] Zhao W and Nomura K 2016 Copolymerizations of norbornene and tetracyclododecene with α-olefins by half-titanocene catalysts: efficient synthesis of highly transparent, thermal resistance polymers *Macromolecules* **49** 59–70
[71] Hong M, Yang G F, Long Y Y, Yu S and Li Y S 2013 Preparation of novel cyclic olefin copolymer with high glass transition temperature *J. Polym. Sci.* A **51** 3144–52
[72] Dallaev R, Pisarenko T, Papež N, Sadovský P and Holcman V 2023 A brief overview on epoxies in electronics: properties, applications, and modifications *Polymers* **15** 3964
[73] Xie Y, Hill C A S, Xiao Z, Militz H and Mai C 2010 Silane coupling agents used for natural fiber/polymer composites: a review *Composites* A **41** 806–19
[74] Singh K, Nanda T and Mehta R 2017 Compatibilization of polypropylene fibers in epoxy based GFRP/clay nanocomposites for improved impact strength *Composites* A **98** 207–17
[75] Garcia-Gonzalez D, Rusinek A, Bendarma A, Bernier R, Klosak M and Bahi S 2020 Material and structural behaviour of PMMA from low temperatures to over the glass transition: quasi-static and dynamic loading *Polym. Test.* **81** 0–18
[76] Yan Y, Sun Y, Su J, Li B and Zhou P 2023 Crazing initiation and growth in polymethyl methacrylate under effects of alcohol and stress *Polymers* **15** 1375
[77] Atzemoglou A A 2025 Development of low temperature activated aryl azide adhesion promoters as versatile surface modifiers *PhD Thesis* ETH Zürich https://doi.org/10.3929/ethz-b-000701943